EXPERIMENTAL INVESTIGATION OF THE INELASTIC BEHAVIOR OF STRUCTURES ISOLATED USING FRICTION PENDULUM BEARINGS

A. Tsiavos[1], D. Schlatter[2], T. Markic[3], B. Stojadinovic[4]

[1] PhD Candidate, ETH, Zurich, Stefano-Franscini-Platz 5, 8093, tsiavos@ibk.baug.ethz.ch

[2] Graduate Student, ETH, Zurich, Stefano-Franscini-Platz 5, 8093, schldavi@student.ethz.ch

[3] PhD Student, ETH, Zurich, Stefano-Franscini-Platz 5, 8093, markic@ibk.baug.ethz.ch

[4] Professor, ETH Zurich, Stefano-Franscini-Platz 5, 8093, stojadinovic@ibk.baug.ethz.ch

Abstract

Current US and European seismic design codes limit the magnitude of strength reduction allowed for seismically isolated structures, thus effectively leading to the elastic design of these structures. This study is focused on the experimental investigation of the behavior of seismically isolated structures when they behave inelastically.

The experimental investigation performed in this study is based on the response of a reduced-scale seismically isolated steel structure to strong analytical pulses and recorded ground motion accelerations applied using the shaking table of the ETH Zurich IBK Structural Testing Laboratory. The part of the structure designed to develop inelastic behavior is a pair of steel coupons that can be easily replaced after such damage. The structure is seismically isolated using four friction pendulum bearings designed to accommodate the large displacements induced by strong ground motion excitations. The bearings are made by MAGEBA SA.

A relation between the experimentally obtained strength and displacement ductility of inelastic seismically isolated structures is presented in this paper. The influence of design parameters, such as the fundamental vibration period of the isolated superstructure, and the types of ground motion is quantified and presented. The experimentally obtained data is compared to an analytically derived strength-ductility-period relation for seismically isolated structures. This comparison will serve to validate the proposed analytical relation and to further the understanding of the behavior of inelastic seismically isolated structures.

Keywords: Experimental investigation of base-isolated structures, Inelastic behavior of base-isolated structures

1. Introduction

The behavior of various types of seismic isolation bearings has been numerically simulated [1-4] and experimentally tested [5-6] to validate the performance of the designed seismically isolated structures subjected to different types of ground motion excitation [7]. In most cases, the isolated superstructures are designed to respond in the elastic range.

The performance of base-isolated structures when the superstructure enters the inelastic range is less well understood. Such inelastic behavior of base-isolated structures is not only theoretical, but can occur in two cases. First, the seismic forces acting on an existing base-isolated structure could exceed the design forces due to, for example, a ground motion stronger than the design ground motion level, or unintentional construction of a weak superstructure. Second, the base-isolated superstructure may be intentionally designed to enter its inelastic response range for design-basis ground motions to reduce their cost and thereby offset the cost of the seismic isolation system.

Constantinou and Quarshie [8], Ordonez et al. [9], Kikuchi et al. [10], Thiravechyan et al. [11] and Cardone et al. [12] investigated the response of inelastic seismically isolated structures and agreed that allowing seismically isolated structures to yield requires careful consideration. Vassiliou et al. [13-15] concluded that designing typical seismically isolated structures to behave elastically, as prescribed by current seismic design codes, is not overly conservative but a necessity that emerges from the fundamental dynamics of such structures.

This elastic design approach, which prohibits extensive yielding of the isolated superstructure, is embedded in the design codes worldwide. The Eurocode [16] allows a maximum behavior factor value of 1.5 for seismically isolated buildings. US ASCE 7 [17] allows the strength reduction factor for a seismically isolated structure to be 0.375 times the one for a corresponding fixed-base structure and no larger than 2. The practical consequence of the elastic design approach is that the base-isolated buildings are designed for forces equal or larger than the design forces for the same fixed-based buildings. The increased cost of the superstructure added to the base isolation system costs represents a serious obstacle to wider adoption of seismic isolation in design and construction practice. Possible inelastic design of the isolated superstructures could decrease the construction costs. However, such design approach would allow for some damage in the superstructure during a design-basis earthquake event. This study quantifies the extent of such damage in terms of displacement ductility demand for the isolated superstructure, thus providing a rational basis for an engineer to choose between an elastic or an inelastic design of the isolated superstructures. This choice should be made accounting for the construction cost of the structure and the expected damage and losses in a design-basis earthquake scenario.

The goal of this study is the experimental investigation of the inelastic behavior of base-isolated structures subjected to strong ground motion excitation. The damage of the isolated superstructure with fixed-base period T_n and isolated period T_b is quantified by its ductility demand μ. The relation between the strength reduction factor of the superstructure R_y and the ductility demand μ is determined and compared to the analytically derived R_y-μ-T_n relations for seismically isolated structures [13].

2. Dynamic modelling

The dynamics of a base-isolated structure, following to the work of Naeim and Kelly [18], is investigated using a two-degree-of-freedom (2-DOF) in-plane model, presented in Fig. 1. The system consisting of the isolation bearings and the isolation base is defined as isolation system. The structure above the isolation system is defined as the isolated superstructure. Masses m_s *and* m_b represent the mass of the isolated superstructure and the mass of the base above the isolation system, respectively. The stiffness and damping are denoted as k_s, c_s, when referring to the superstructure and as k_b, c_b when referring to the base. Horizontal displacement u_s is the relative displacement of the superstructure with respect to the base and u_b is the horizontal displacement of the isolation bearings with respect to the ground. The ground displacement to which the system is subjected is denoted as u_g. The notation used to describe the inelastic response of fixed-base single-degree-of-freedom (SDOF) structures is adopted as follows.
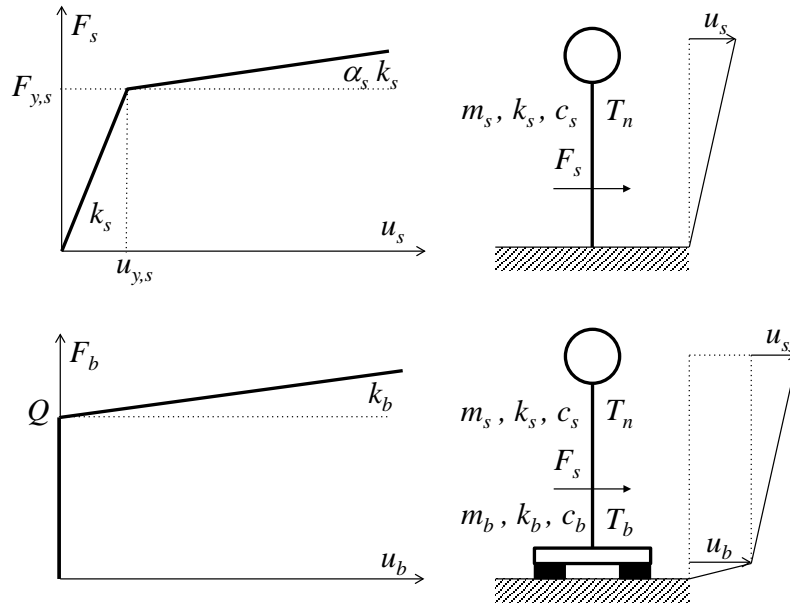
Figure 1: Parameters of the SDOF model of a fixed-base structure and of a 2-DOF model of a base-isolated structure.

The vibration period of the SDOF system is T_n. The displacement ductility ratio μ is defined as:

$$\mu = \frac{u_m}{u_y} \tag{1}$$

where u_m and u_y denote the maximum inelastic displacement and the yield displacement of the SDOF system, respectively. The strength reduction factor R_y is the ratio of the minimum strength required to maintain the SDOF system response in the elastic range, $F_{el,s}$ and the SDOF system yield strength $F_{y,s}$:

$$R_y = \frac{F_{el,s}}{F_{y,s}} \tag{2}$$

The following quantities are defined for the 2-DOF model of the base-isolated structure:

1. Period and cyclic frequency of the isolated superstructure:

$$T_n = 2\pi\sqrt{\frac{m_s}{k_s}} \ , \ \omega_n = \sqrt{\frac{k_s}{m_s}} \tag{3}$$

2. Isolation period and cyclic frequency:

$$T_b = 2\pi\sqrt{\frac{m_s + m_b}{k_b}} \ , \ \omega_b = \sqrt{\frac{k_b}{m_s + m_b}} \tag{4}$$

3. Mass ratio:

$$\gamma_m = \frac{m_s}{m_s + m_b} \tag{5}$$

3. Design of the base-isolated structure

The goal of the design is to obtain a seismically isolated structure with the following design requirements:
1. Activation of the seismic isolation system before yielding of the isolated superstructure.
2. Concentration of the inelastic behavior of the isolated superstructure in a specifically designed element, which can be easily constructed and replaced.
3. The fixed-base period T_n of the superstructure shall resemble the one of a short, couple-of-storey building: 0.3 s $<T_n<$0.5 s
4. The period of the isolated structure shall be roughly five times greater than the one of the fixed base structure ($T_B>5$ T_n), to widely separate the already orthogonal structural and seismic isolation vibration modes.
5. The total mass of the system shall not exceed 1000 kg.
After the conduction of a feasibility study, the following structural system was designed.
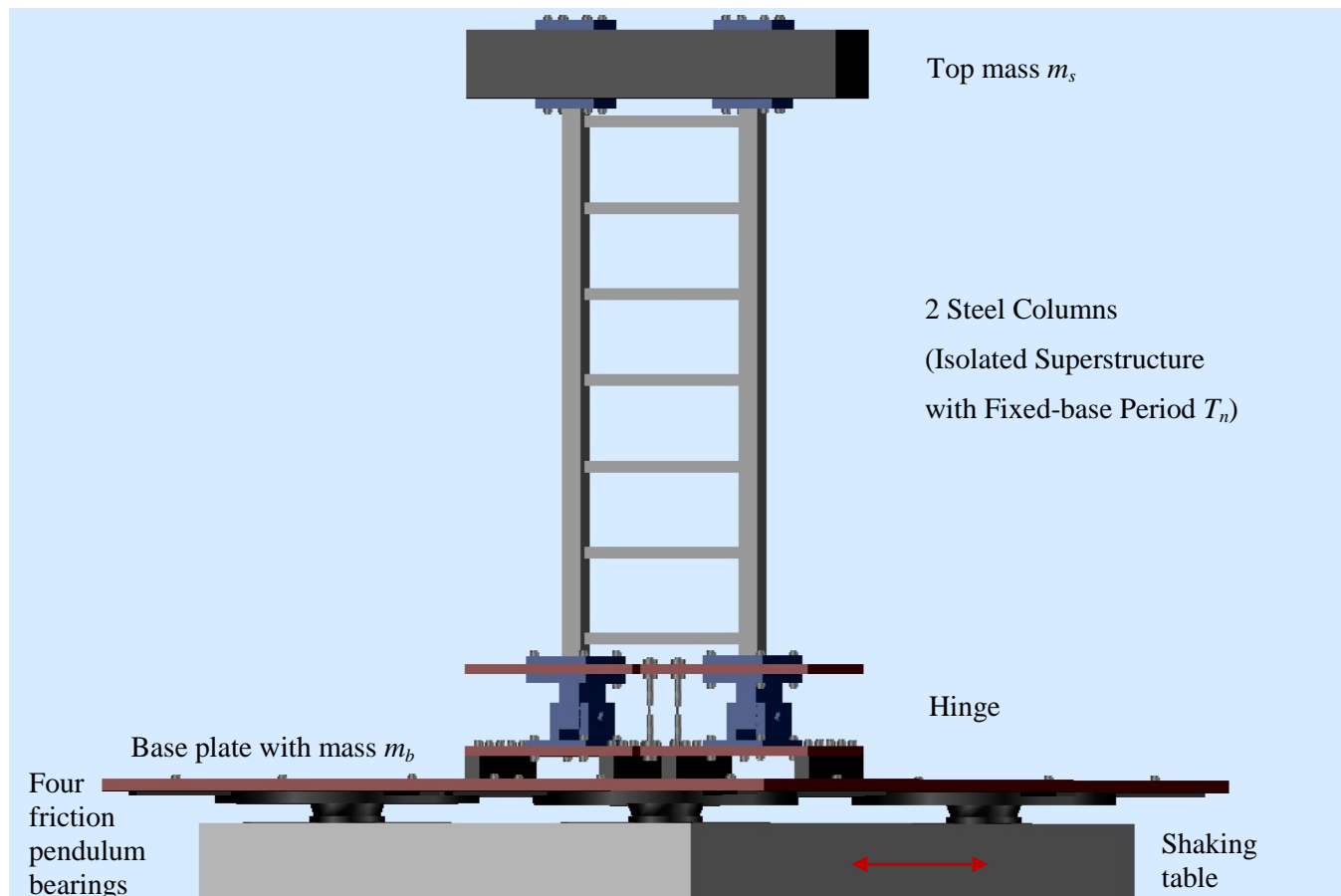
Fig. 2: 3D View of the designed isolated structure with 4 friction pendulum bearings

As shown in Fig. 2, the designed structure is a seismically isolated cantilever structure with a lumped mass m_s attached on the top. The cantilever structural system consists of two vertical steel columns, connected horizontally with 7 stiffening steel beams that guarantee the in-plane behavior of the system under shaking table excitation. The steel beams are anchored to a bottom plate. This plate is supported by two hinge elements (Fig. 2) that allow the rotation of the plate in the plane of the excitation (Red arrow in Fig. 2) and two steel coupons (Fig. 2, 3) that restrain this rotation. These four elements are anchored to another plate, which is supported by the base plate of the isolation system with mass m_b. Both plates above the base plate are equiped with small gaps that allow for the easy replacement of the steel coupons in case of damage. The isolation system consists of 4 friction pendulum bearings, which are distibuted symmetrically on the shaking table. Table 1 shows the dimensions of the components of the isolated structure.

Table 1: Structural components of the designed isolated structure

Part	Material	Quality	Length (mm)	Width (mm)	Thickness (mm)	Height (mm)	Weight (kg)	Radius (mm)
1. Top mass	Steel	S235	750	150	170	-	250	-
2. Column-Superstructure	Steel	S235	1345	2100	10	1600	8	-
3. Base plate	Steel	S235	2.5	2.5	30	-	665	-
4. Bearing	Steel	S235	-	-	-	-	75	1500
5. Shaking Table	Steel	S235	1000	2000	-	-	-	-
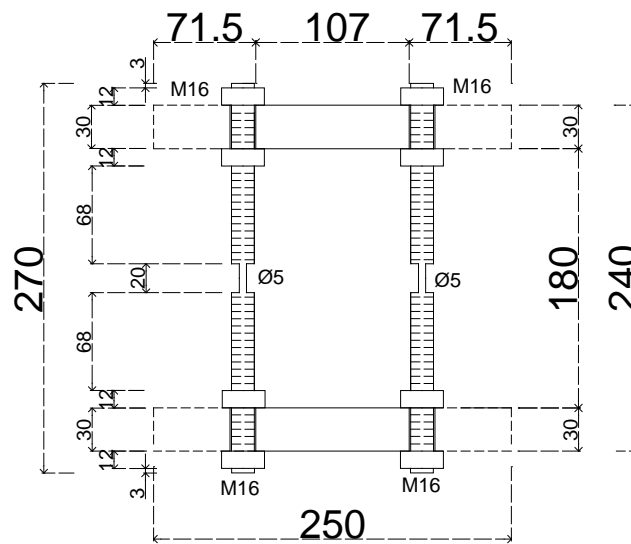
Fig. 3: Elevation view of the 2 steel coupons (Dimensions in mm, Steel quality S275)

The design yield strength of the structure is F_y=435 N and the design yield strength of the isolation system is Q=1027 N. The design fixed-base period of the structure is T_n=0.42 s and the post-yielding isolation period is T_b=2.46 s. The friction coefficient μ_f of the bearings is 0.105.

4. Constructed structure

The designed structural system was constructed at the ETH Zurich IBK Structural Testing Laboratory and is shown in Fig. 4. The isolators are made by MAGEBA SA as the small version of their RESTON Pendulum Type Mono isolator. The fixed-base period of the constructed structure is T_n=0.52 s, as measured in a free vibration test. The post-yielding isolation period T_b=2.3 s was determined using a sine sweep shaking table excitation. The measured value of the yield strength of the isolation system is Q=520 N. The differences stem from the inevitable discrepancies between the nominal and the actual mechanical properties of the components. The mass ratio of the constructed structure is γ_m=0.2. Two different diameters have been used for the reduced-diameter middle part of the steel coupons shown in Fig. 3, one of d=4 mm and one of d=5 mm.

Fig. 4: Constructed isolated structure in the ETH laboratory

5. Ground motion response data

The structure shown in Fig. 4 was excited by 4 different ground motion excitations taken from the PEER Center ground motion database [19]: 1) 35% acceleration-scaled 1971 San Fernando PCD164 ground motion record, recorded at the 279 Pacoima Dam station; 2) 75% acceleration-scaled 1994 Northridge 0637-270 ground motion record, recorded at the USGS/VA 637 LA-Sepulveda VA Hospital station, 3) Unscaled 1983 Coalinga D-TSM270 ground motion record, recorded at the 1651 Transmitter Hill station and 4) 32.5% acceleration-scaled 1978 Tabas TAB-LN ground motion record, recorded at the 9101 Tabas station.

5.1 Response to the 35% 1971 San Fernando ground motion excitation

The applied scaled-down 1971 San Fernando ground motion shown in Fig. 5 has a PGA of 0.429g.
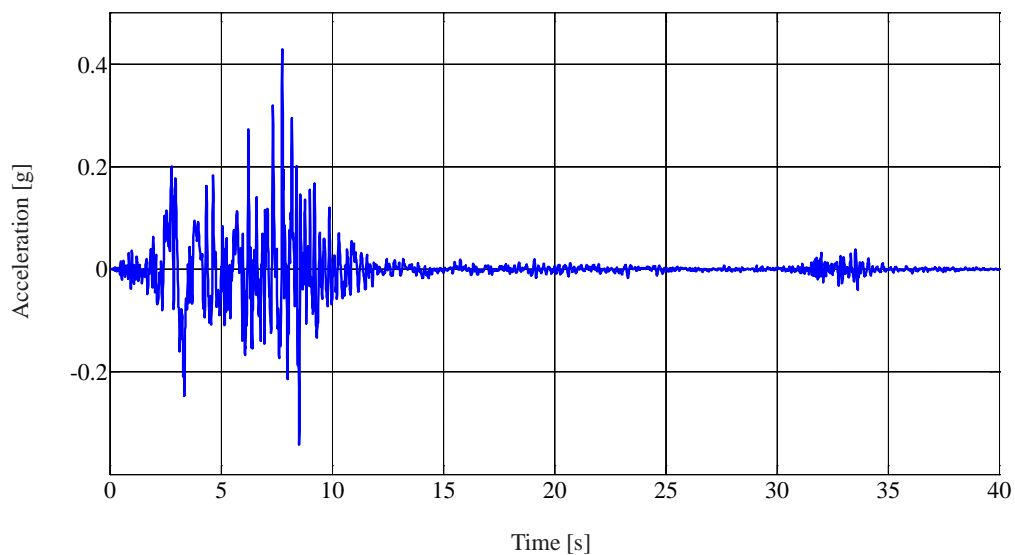
Fig. 5: 35%-scaled 1971 San Fernando ground motion excitation

The relative displacement time history of the top mass with respect to the base plate and the relative displacement time history of the base plate with respect to the shaking table are shown in Fig. 6. The hysteretic force-displacement loop for the superstructure is shown in Fig. 7.
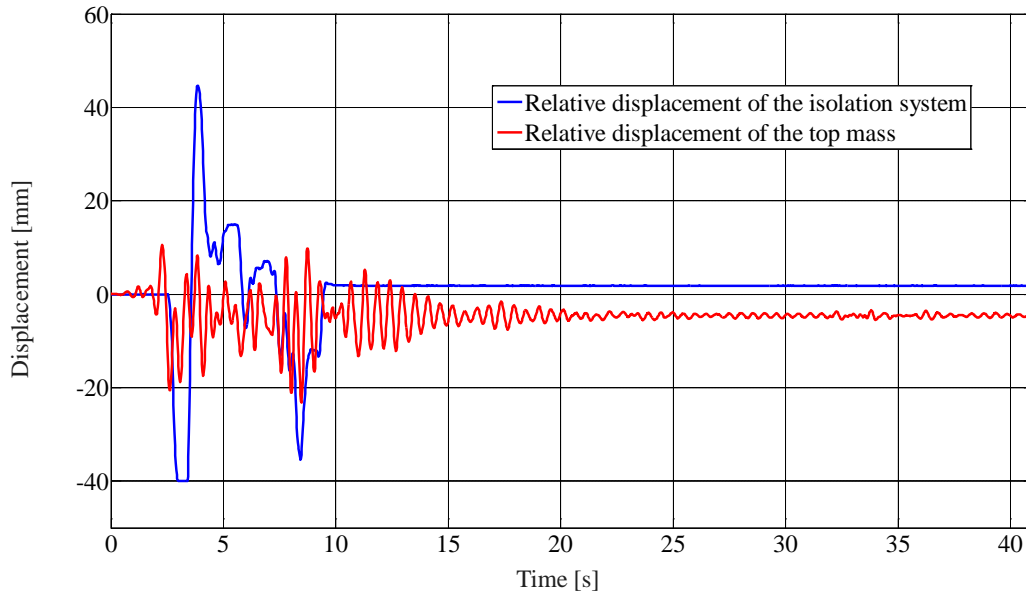
Fig. 6: Displacement time history response to the 35% 1971 San Fernando ground motion

The maximum recorded displacement of the superstructure for this motion was 23.2 mm. Given the actual yield deformation and strength of the steel coupons, as well as the elastic deformation of the superstructure, this displacement corresponds to a displacement ductility μ=1.6, and the measured forces indicate that the strength reduction factor R_y=1.9. The elastic force in the superstructure for each ground motion excitation was computed analytically by using the experimentally derived properties of the isolators and the isolated superstructure. The maximum displacement of the isolators was 44.7 mm.
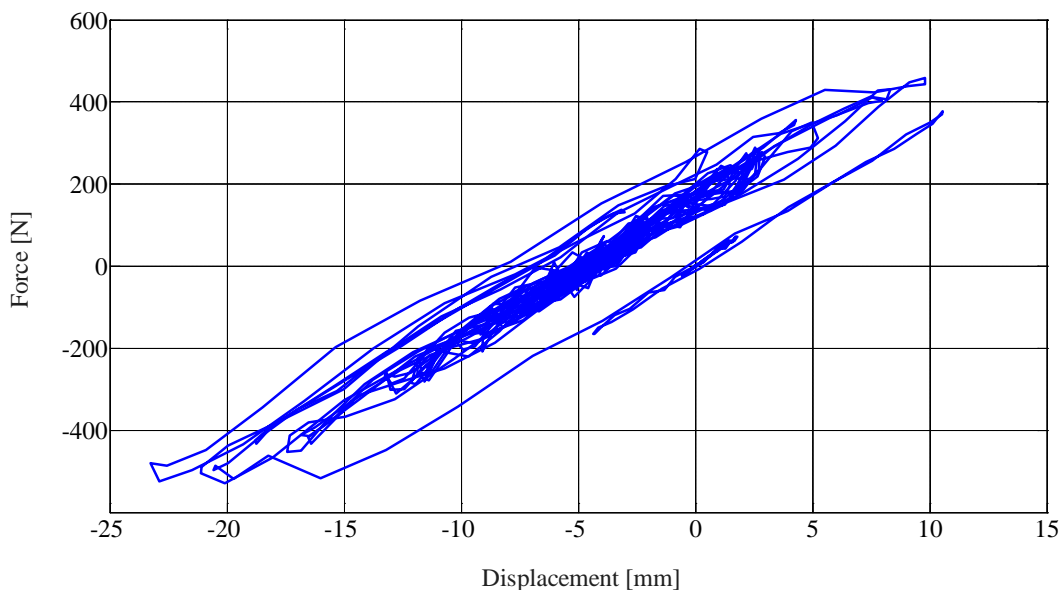
Fig. 7: Force-Displacement response of the superstructure to the 35% 1971 San Fernando ground motion

7

5.2 Response to the 32.5% 1978 Tabas ground motion excitation

The applied scaled-down 1978 Tabas ground motion shown in Fig. 8 has a PGA of 0.27g.
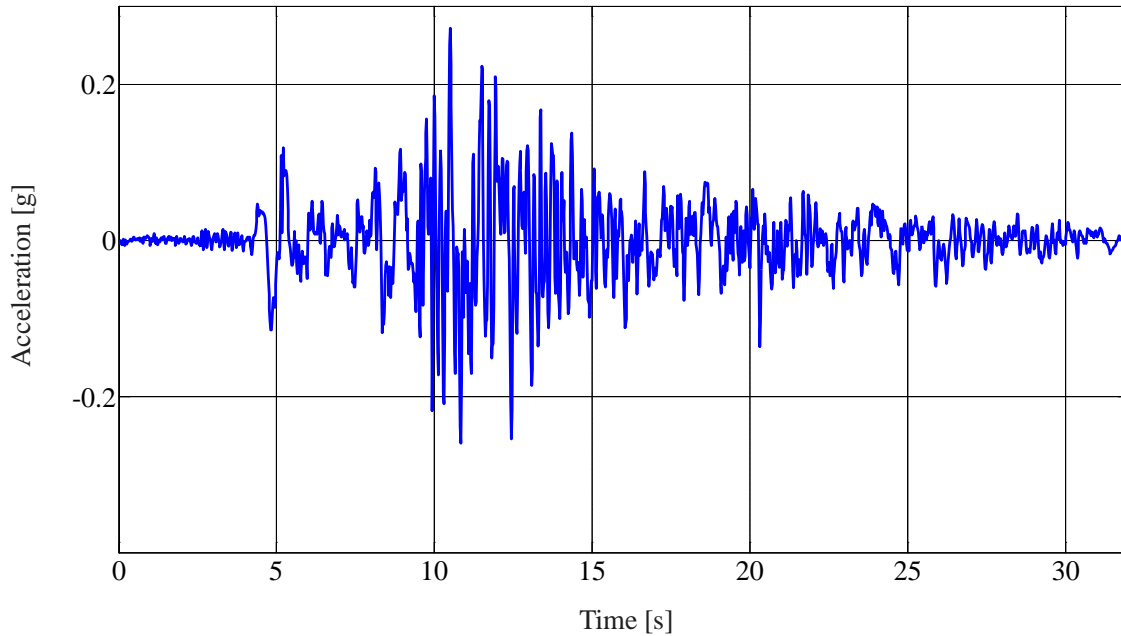
Fig. 8: 32.5%-scaled 1978 Tabas ground motion excitation

The relative displacement time history of the top mass with respect to the base plate and the relative displacement time history of the base plate with respect to the shaking table are shown in Fig. 9. The hysteretic force-displacement loop for the superstructure is shown in Fig. 10. Significant yielding of the coupons was observed.
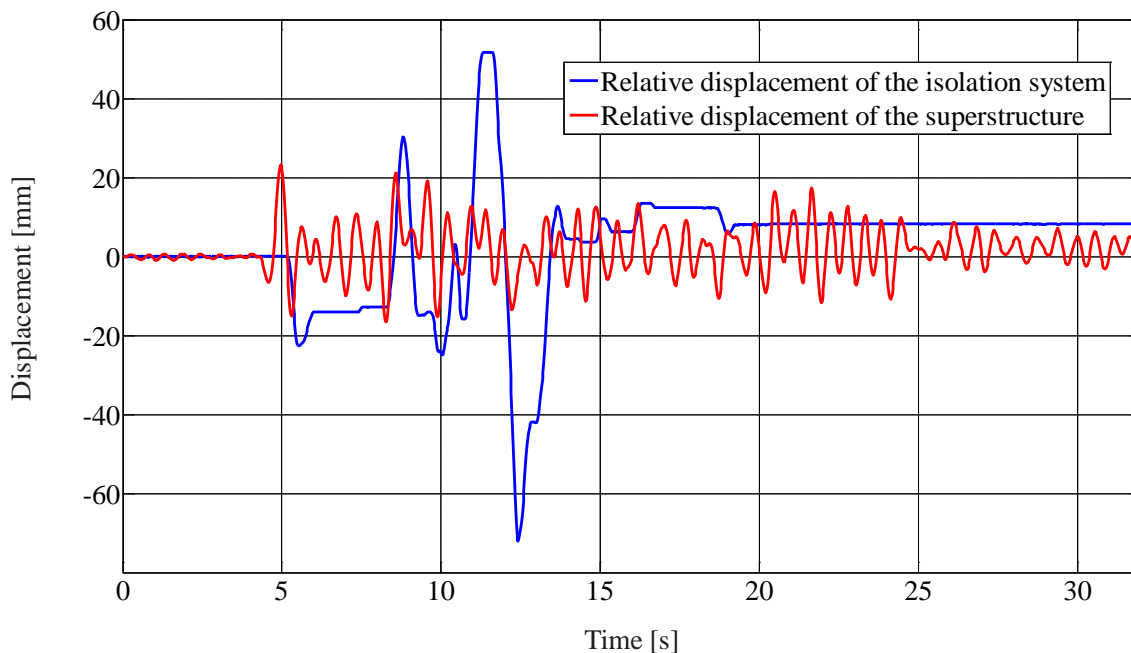
Fig. 9: Displacement time history response to the 32.5% 1978 Tabas ground motion

8
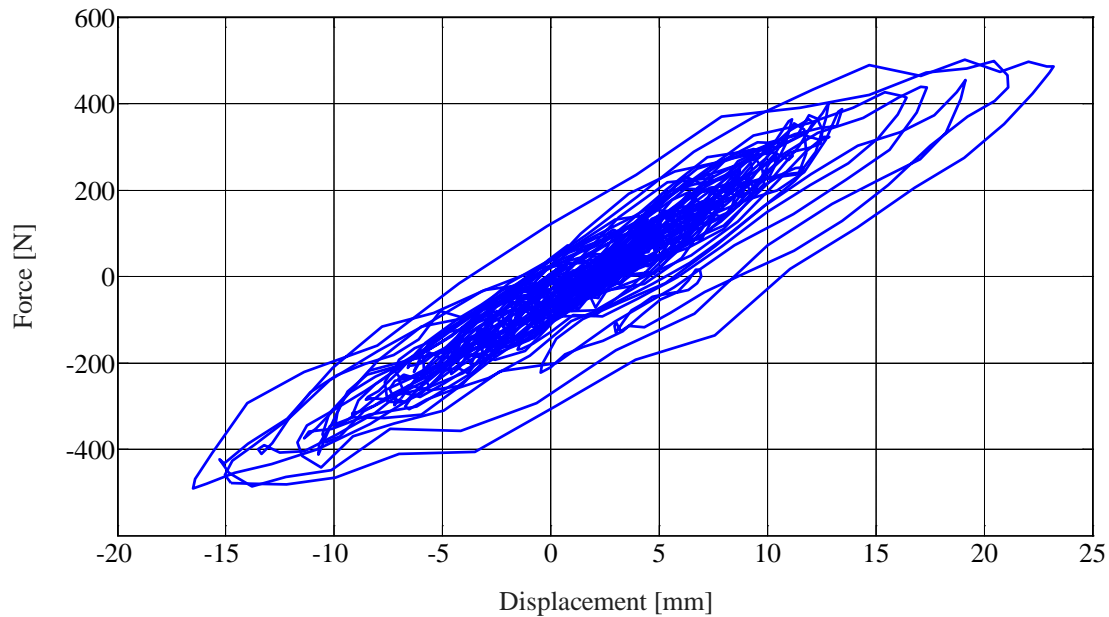
Fig. 10: Force-Displacement response of the superstructure to the 32.5% 1978 Tabas ground motion

The maximum recorded displacement of the superstructure for this motion was 23.2 mm. Given the actual steel coupon mechanical properties, this displacement correspond to a displacement ductility $\mu=1.7$. The strength reduction factor $R_y=1.7$. The maximum displacement of the isolators was 72 mm. Significant yielding of the coupons and residual displacement of the isolators are observed.

5.3 Response to the unscaled 1983 Coalinga ground motion excitation

The applied unscaled 1983 Coalinga ground motion shown in Fig. 11 has a PGA of 0.84g.
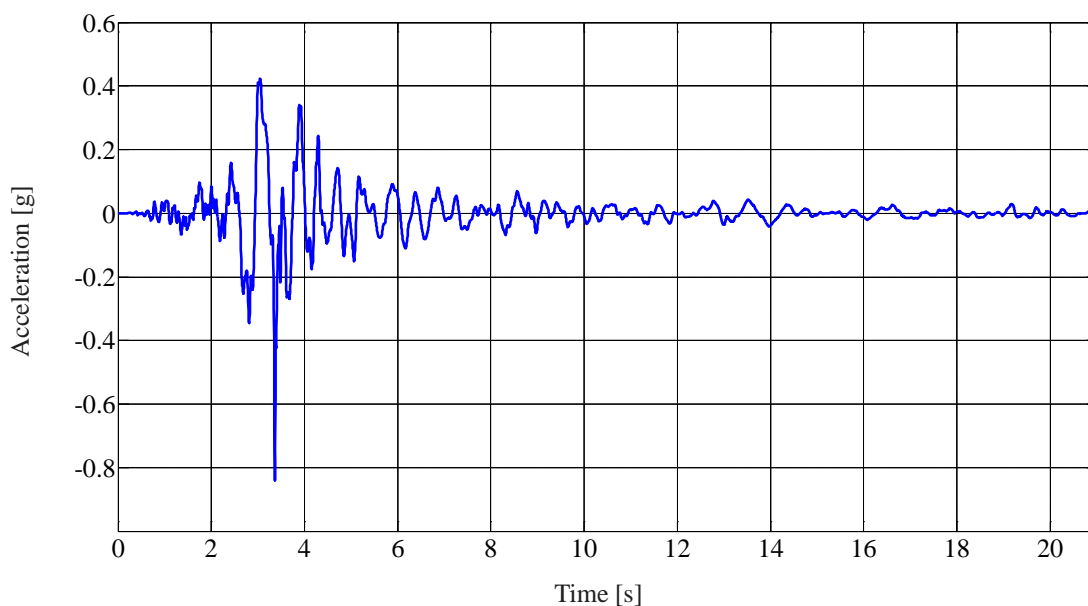
Fig. 11: Unscaled 1983 Coalinga ground motion excitation

The relative displacement time history of the top mass with respect to the base plate and the relative displacement time history of the base plate with respect to the shaking table are shown in Fig. 12. The hysteretic force-displacement loop for the superstructure is shown in Fig. 13.
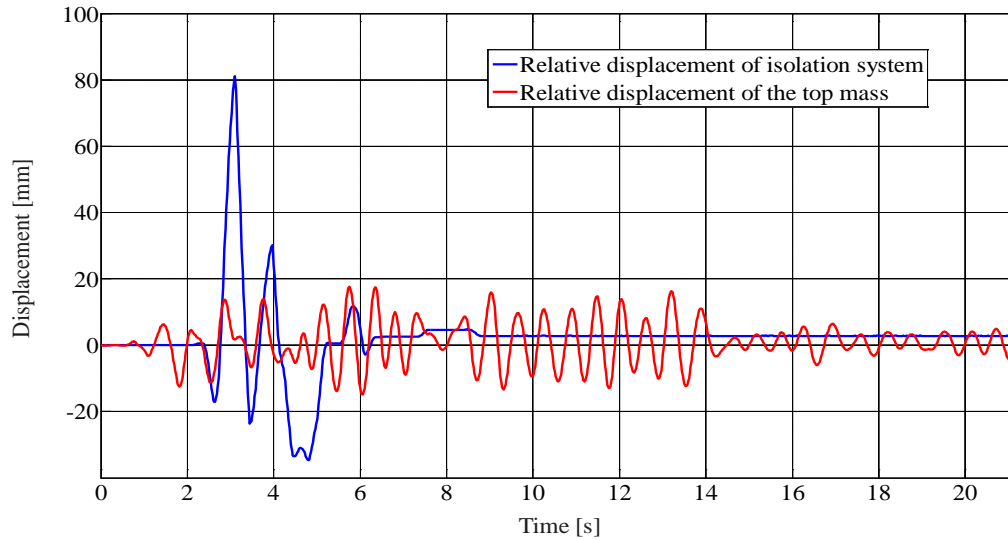
Fig. 12: Displacement time history response to the unscaled 1983 Coalinga ground motion
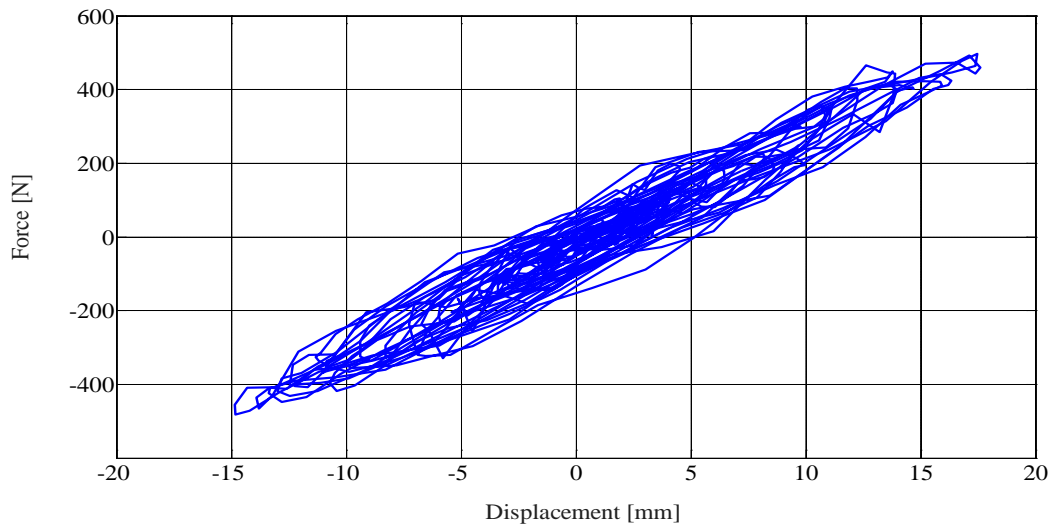
Fig. 13: Force-Displacement response of the superstructure to the unscaled 1983 Coalinga ground motion

The maximum recorded displacement of the superstructure for this motion was 17.6 mm. Given the actual mechanical properties of the steel coupons, this displacement corresponds to a displacement ductility μ=1.3. The strength reduction factor R_y=1.6. The maximum displacement of the isolators is 81.1 mm.

6. Comparison to the analytically derived R_y-μ-T_n relations

The R_y-μ-T_n data extracted from the ground motion excitations of the isolated structures are compared to the analytically derived median R_y-μ-T_n relations for a mass ratio γ_m=0.2 by Tsiavos et al. [13] for a wide ensemble of ground motion excitations. The comparison is shown in Fig. 14. The R_y-μ-T_n relations derived by Newmark et al. [20] and Vidic et al. [21] for fixed-base structures and the proposed R_y-μ-T_n relations derived by Tsiavos et al. [13] for isolated superstructures with γ_m=0.9 are shown on the same figure.

10
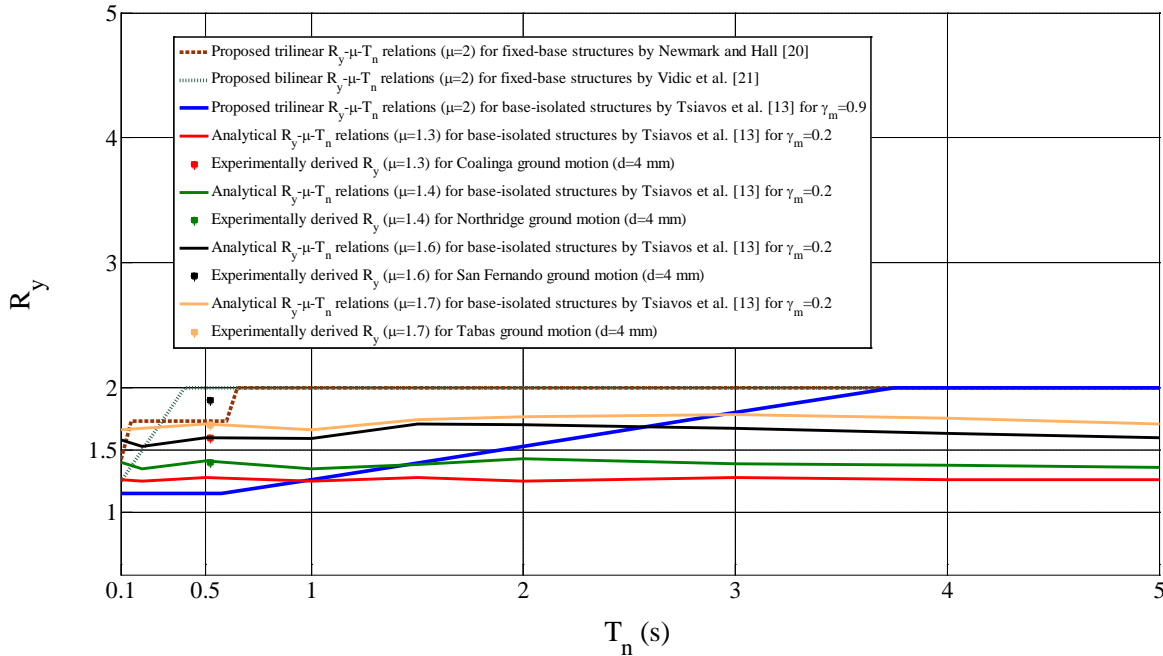
Fig. 14: Comparison of the analytical and experimental data

As shown in the Fig. 14, the data obtained from the 35% 1971 San Fernando, the unscaled Coalinga and the Tabas ground motion test are in good agreement with the analytically derived R_y-μ-T_n relations [13]. The relations are not conservative for the 75% 1994 Northridge ground motion excitation, as they indicate a slightly larger value of the design yield strength reduction factor for the same ductility demand μ. However, the difference in this case can be attributed to the discrepancy between the ground motion record and the applied input motion due to the velocity limitation of the shaking table.

The strength reduction factor R_y values obtained in this experiment are, in most of the cases, lower than the proposed values for fixed-base structures by Newmark and Hall [20] and Vidic et al. [21]. This difference indicates that the R_y-μ-T_n relations for fixed-base structures are not conservative as they underestimate the strength of base-isolated structures required to keep their deformations within limits expected for fixed-base structures. However, the proposed R_y-μ-T_n relations for base-isolated structures [13] are conservative and can be used for the design of new and evaluation of existing base-isolated structures.

7. Conclusions

A small-scale specimen and experimental setup were designed and built to allow for an investigation of the inelastic behavior of base-isolated structures. The behavior of the isolated superstructure is governed by the inelastic response of the easily replaceable steel coupons. This makes it possible to conduct a large number of parametric tests.

Data from four typical experiments is presented in this paper. The data indicate that although the tested structures were designed to remain elastic, they can easily enter their inelastic behavior range when they are excited by a strong ground motion excitation.

The analytically derived R_y-μ-T_n relations [13] are in most of the cases conservative when compared to the experimental data. They can be used to design of new base-isolated structures or to evaluate the seismic performance of existing base-isolated structures subjected to strong ground motion excitations. The main reasons for the differences between the analytical and experimental data are attributed to the velocity limitation of the shaking table.

8. References

[1] Constantinou MC, Mokha A, Reinhorn A (1990) Teflon bearings in base isolation. II: Modeling. *Journal of Structural Engineering (ASCE)*, **116**(2):455–474.

[2] Mosqueda G, Whittaker AS, Fenves GL (2004) Characterization and modeling of friction pendulum bearings subjected to multiple components of excitation. *Journal of Structural Engineering (ASCE)*, **130**(3):433–442.

[3] Yang TY, Konstantinidis D, Kelly JM (2010) The Influence of Isolator Hysteresis on Equipment Performance in Seismic Isolated Buildings. *Earthquake Spectra*, **26** (1), 275-293.2.

[4] Fenz DM, Constantinou MC. (2008) Spherical sliding isolation bearings with adaptive behavior: theory, *Earthquake Engineering and Structural Dynamics,* **37**(2):163–183.

[5] Becker TC, Mahin SA (2012) Experimental and analytical study of the bi-directional behavior of the triple friction pendulum isolator. *Earthquake Engineering and Structural Dynamics*, **41**(3):355–373.

[6] Dao ND, Ryan KL, Sato E, Sasaki T. (2013) Predicting the displacement of triple pendulum™ bearings in a full-scale shaking experiment using a three-dimensional element. *Earthquake Engineering and Structural Dynamics,* **43**: 1683–1701.

[7] Shi Y, Kurata M, Nakashima M. (2014) Disorder and damage of base-isolated medical facilities when subjected to near-fault and long-period ground motions, *Earthquake Engineering and Structural Dynamics,* **43**(11):1683–1701.

[8] Constantinou MC, Quarshie JK (1998) Response modification factors for seismically isolated bridges. *Report No. MCEER-98-0014, Multidisciplinary Center for Earthquake Engineering Research*, Buffalo, NY

[9] Ordonez D, Foti D, Bozzo L. (2003) Comparative study of the inelastic response of base isolated buildings. *Earthquake Engineering and Structural Dynamics,* **32**:151–164.

[10] Kikuchi M, Black CJ, Aiken ID (2008) On the response of yielding seismically isolated structures. *Earthquake Engineering and Structural Dynamics*, **37**(5):659–679.

[11] Thiravechyan P, Kasai K, Morgan TA (2012) The effects of superstructural yielding on the seismic response of base isolated structures., *Joint Conference proceedings, 9th International Conference on Urban Earthquake Engineering / 4th Asia Conference on Earthquake Engineering, Tokyo*, Japan, 1451-1458.

[12] Cardone D, Flora A, Gesualdi G. (2013) Inelastic response of RC frame buildings with seismic isolation. *Earthquake Engineering and Structural Dynamics*, **42**:871–889.

[13] Tsiavos A, Vassiliou MF, Mackie KR and Stojadinovic B (2013) R-μ-T relationships for seismically isolated structures, *COMPDYN 2013, 4th International Conference on Computational Methods in Structural Dynamics and Earthquake Engineering*, Kos Island, Greece, 12-14 June.

[14] Tsiavos A, Vassiliou MF, Mackie KR and Stojadinovic B (2013) Comparison of the inelastic response of base-isolated structures to near-fault and far-fault ground motions, *VEESD 2013, Vienna Congress on Recent Advances in Earthquake Engineering and Structural Dynamics & D-A-CH Tagung,* Vienna, Austria, 28-30 August

[15] Vassiliou MF, Tsiavos A and Stojadinovic B (2013) Dynamics of Inelastic Base Isolated Structures Subjected to Analytical Pulse Ground Motions, *Earthquake Engineering and Structural Dynamics*, **42** (14), 2043-2060.

[16] CEN (2004), *Eurocode 8, Design of structures for earthquake Resistance—Part 1: general rules, seismic actions and rules for buildings*. EN 1998-1:2004. Comité Européen de Normalisation, Brussels.

[17] Structural Engineering Institute (2010). Minimum design loads for buildings and other structures (Vol. 7, No. 5). ASCE.

[18] Kelly JM (1997) *Earthquake Resistant Design with Rubber*. Springer: London,.

[19] PEER NGA strong motion database (2010), Pacific Earthquake Engineering Research Center, Berkeley, California (http://peer.berkeley.edu/nga/ on 08.09.2014).

[20] Newmark NM, Hall WJ (1973) Seismic design criteria for nuclear reactor facilities, *Report 46*, Building Practices for Disaster Mitigation, National Bureau of Standards, pp. 209–236.

[21] Vidic T, Fajfar P, Fischinger M (1994) Consistent inelastic design spectra: strength and displacement, *Earthquake Engineering and Structural Dynamics,* **23**, 502–521